Published in final edited form as:
Langmuir. 2009 January 20; 25(2): 653–656. doi:10.1021/la803369j.

Effect of Monomer Structure and Solvent on the Growth of Supramolecular Nano-Assemblies on a Graphite Surface

Aryavarta M. S. Kumar[†], **Justin D. Fox**[‡], **Lauren E. Buerkle**[‡], **Roger E. Marchant**[*,†,‡], and **Stuart J. Rowan**[*,‡,†,§]

†*Department of Biomedical Engineering, Case Western Reserve University, Cleveland, OH 44106*

‡*Department of Macromolecular Science and Engineering, Case Western Reserve University, Cleveland, OH 44106*

§*Department of Chemistry, Case Western Reserve University, Cleveland, OH 44106*

Abstract

The self-assembly of high aspect ratio hierarchical surface assemblies, as observed by fluid tapping mode AFM, can be achieved through careful design of the supramolecular interactions between low molecular weight adsorbates. Needle-like assemblies of monotopic guanine end-capped alkanes grow on a graphite surface when deposited from a water:DMSO solution. The growth of these assemblies can be monitored by AFM in "real time" and the growth rate along the two different axes can be understood (through molecular modeling) in terms of the specific adsorbate-adsorbate interactions along those axes. Additionally, through judicious solvent selection (e.g. use of non-H-bonding solvents such as *o*-dichlorobenzene), which allow formation of hydrogen bonding aggregates in solution and influence the surface-adsorbate interactions, dramatically different surface assemblies of these guanine derivatives are obtained.

Introduction

Supramolecular chemistry at the interface holds great promise for the facile access to new nanostructures using the "bottom up" approach.[1,2] The design of new self-assembled surface patterns requires an understanding of both adsorbate-adsorbate and surface-adsorbate interactions. For example, amphiphilic, monotopic molecules consisting of hydrogen bonding (H-bonding) polar head groups and n-alkyl tails, are known to spontaneously assemble on a surface in a head-to-head / tail-to-tail fashion in which the adsorbate-adsorbate interactions such as alkyl-alkyl[3] and H-bonding play a key role.[4] Surface-adsorbate interactions can also play a critical role in controlling the nature of the self-assembly. For example, n-alkanes are known to epitaxially order on graphite surfaces.[5] By controlling both sets of interactions, researchers have begun to explore the potential of molecules to form controllable nanoarchitectures. [4,6] Using a series of guanine derivatives (Figure 1a, **1–4**) we report herein studies which show how drastically different molecular surface assemblies can be accessed at the liquid/solid interface by either tailoring the nature of the adsorbate-adsorbate and/or the adsorbate-substrate interactions through molecular design and/or solvent choice. Furthermore, we are able to follow the growth of some of these assemblies at the liquid/surface interface through real-time monitoring using fluid tapping mode AFM.

In recent years, a number of groups have carried out studies on how different nucleobases and nucelobase pairs self-assemble on a surface. These studies have primarily focused on the

Corresponding Authors: Tel: 216 368 4242 (sjr); 216 368 3005 (rm). e-mail: stuart.rowan@case.edu; roger.marchant@case.edu.

assembly of the underivatized nucleobases (adenine, cytosine, guanine, thymine and uracil), which have either been deposited using ultrahigh vacuum techniques, from solution, or have been studied directly at the organic liquid/solid interface.[7,8,9] We have recently been interested in the assembly of a range of more complex guanine derivatives deposited onto highly oriented pyrolytic graphite (HOPG) from aqueous solutions. We reported[10] that homoditopic guanine end-capped *n*-alkanes (e.g. **4**) deposited from water:DMSO solutions form molecular-sized epitaxially ordered bands on HOPG. It was hypothesized that the mechanism of assembly involved the monomers adsorbing and then rearranging on the surface to form the nano-sized linear bands (aided by H-bonding and epitaxy). From modeling, it was proposed that the guanines form a double-stranded tape motif (Figure 1b, Tape I) in which Watson-Crick (W/C) H-bonded dimers extend the polymeric aggregate (x-axis, Figure 1b), and inter-chain guanine H-bonds (*, Figure 1b) form between the exo-NH_2 and N-7 on the Hoogsteen face of adjacent guanines (y-axis, Figure 1b). These monomers form complete surface assemblies (at 28 °C and >30 nM) in <5 mins (before the first AFM scan). It was hypothesized that the fast growth rate was partially on account of H-bonding controlling the adsorbate-adsorbate interactions along both axes. We therefore rationalized that by reducing the strength of the molecular interactions along one axis, it would be possible to access anisotropic hierarchical nano-assemblies.[11]

In a first attempt to test this hypothesis, the monotopic guanine end-capped n-dodecane (**1**) was targeted. The rate of growth of **1** along the y-axis in Figure 1b should be determined by inter-chain (*) nucleobase H-bonding, similar to the growth of the ditopic derivatives. However, as a result of the monotopic nature of **1**, the H-bonded aggregates via the Watson-Crick (W/C) face of the guanines are limited to dimers along the x-axis. Thus formation of extended aggregates along this axis would require the use of weaker alkyl-alkyl interactions.

A DMSO solution of the monotopic **1** was introduced into a water droplet on HOPG at 28 °C and diluted to 49:1 water:DMSO (~10–20 nM). Using AFM fluid tapping mode, a monolayer consisting of linear bands with widths of 5.4 ± 0.1 nm (Figure 1c) was observed immediately upon imaging. Molecular modeling provided insight into the nature of these assemblies. The models, in which **1** assembles using the Tape I motif (Figure 1b) with no alkyl tail interdigitation, correctly predict band widths of 5.5 nm (Figure 1d). Models minimized using other known guanine tape motifs[9] (see Supp. Info.) had widths (4.1, 4.4 nm) that do not match the AFM data and had higher modeled energies. Comparison of the AFM data and the molecular model suggest that the length of the molecules run parallel to the x-axis. Unfortunately, on account of the quality of the AFM data, no periodicity could be observed along the y-axis. The models however, suggest that the y-axis spacing is controlled by the H-bonding motif which has a repeat distance of ca. 8 Å and is too small to allow alkyl tail interdigitation;the van der Waals radii of alkyl tail atoms overlap if Tape I is intact and interdigitation occurs.

Self-assembly of **1** at lower concentrations (<10 nM) shows the formation of high aspect ratio needle-like assemblies (Figure 2a) consistent with different rates of growth along the x and y axes. These needles were as large as 6 μm in length with aspect ratios ranging from as low as 4 to as high as >50.5.4 nm bands run parallel to the length of the needle assembly within all these needle-like structures with each needle assembly arranged epitaxially when compared to other needles. In order to examine the effect of the monotopic verses ditopic architecture of the monomers, sub-monolayer assemblies of the ditopic monomer **4** were also studied (Figure 2b) by using much lower concentrations (0.2 nM) of **4** than those we previously reported (10–20 nM).[10] These assemblies appear dramatically different from those observed for **1**, exhibiting much lower aspect ratios.

To further understand the relative initial growth rate of assemblies formed from the monotopic **1** along both axes, *in situ* AFM scans of surface domain growth were captured. Figure 3 a–c shows a series of AFM images, using 2 × 2 μm scan sizes, which capture the growth of one of the needle-like assemblies. The images clearly demonstrate the anisotropic nature of the growth. Figure 3d shows a magnified image of this assembly comprised of 5.4 nm wide bands. From a series of seven similar experiments (see Supp. Info.) the average ratio of y (length of the needle assemble) to×(width of the needle assembly) growth rate, R_{yx}, was estimated to be ca. 150 ± 60, although it should be noted that the rate of nucleation and growth, as expected, will be dependent on a number of factors including temperature, concentration, the water:DMSO ratio and presumably the influence of the tip (vide infra). Thus the actual value of R_{yx} reported should be interpreted with care and is used here only to highlight the anisotropic nature of the assembly growth. It is worthy to note that the growth in the width of the needle (x-axis) generally occurs via multiple nucleation sites along the length of the needle (e.g. Figure 3d) which merge together to form a complete band rather than one nucleation site which then grows the length of the assembly. Further AFM experiments monitoring the growth at smaller scan sizes (500 × 500 nm) (e.g. Figure 3e–h) again clearly show the faster y-axis growth of the needle-like assembly. In this particular experiment the x-axis growth rate was 8.1 nm/min while the y-axis growth rate was 12 nm/min from one end of the assembly. Using the models and assuming y-axis growth occurs at the same rate at both ends of the assembly, the growth rate along the x- and y-axes is calculated to be 3 and 30 molecules/min respectively (see Supp. Info.). Thus the R_{yx} from this experiment was only 10. The reduced difference in the two growth rates in this latter experiment is presumably on account of the higher tip force and the horizontal scan direction disrupting the y axis growth at these smaller repeated scan sizes. This highlights the impact the AFM tip can have on these growing assemblies and again emphasizes the caution that needs to be taken when directly comparing growth between different experiments, especially at smaller AFM scan sizes. Furthermore, as can been seen in Figures 3g and h, this particular growing assembly is close to a step edge (that helps as a reference) which presumably also will influence the nature of its growth. None-the-less the slower x-axis growth rate supports the expectation that it is dependent on the weaker alkyl-alkyl interactions, while the growth along the y-axis is dependent on guanine inter-chain H-bonds, presumably resulting in the order(s) of magnitude faster incorporation of molecules into the y-axis of the assembly (compared to the x-axis). It is worthy to note that these experiments are consistent with the formation mechanism of these surface assemblies from aqueous environments occurring through molecular adsorption followed by molecular rearrangement into the hierarchical nano-structured assemblies. It can be expected that at nanomolar concentrations in water:DMSO there will be little to no intermolecular hydrogen bonding in solution and that if hydrogen-bonding does play a role in the assembly process it does so predominately at the HOPG surface.

To better understand the importance of hydrogen bonding in the growth of these assemblies the surface assembly of **2** on HOPG was also investigated (see Supp. Info.). The guanine in **2** is protected by a benzyl carbamate on the exo-amine, significantly reducing the potential for Watson-Crick hydrogen-bonding. No high aspect ratio domains were observed with **2**, although unstable blocky domains could be observed only after AFM scanning was suspended for several hours. This is consistent with hydrogen boding playing a significant role not only in the formation of the high aspect ratio assemblies, but also the stability of the film.

Recently, Giorgi et al.[12] reported that assembly of the related mono-guanosine end-capped alkane (**3a**) on HOPG deposited from trichlorobenzene yielded (as observed by STM) small domains of band structures with repeat distances of 2.2 nm consistent with an assembly formed with the guanine Tape II motif (Figure 4a) and interdigitated alkyl chains. Thus with the goal of trying to understand the reason for the differences in the assemblies of **1** reported herein and the assemblies of derivatives of **3**, a series of additional experiments were performed. One

major difference between these two studies is the nature of the solvent used to deposit the monomers on the HOPG surface. The monotopic guanosine derivative **3b** was, therefore, synthesized and deposited onto HOPG from water:DMSO solutions using a procedure similar to those we previously used for sub-monolayer assembly of **1** (vide supra). Similar to **1**, needle-like domains were observed although this time with 6.1 ± 0.1 nm band widths (Figure 4b,c). As was the case for **1**, molecular modeling suggests that **3b** forms the double stranded Tape I motif with no alkyl interdigitation. However, when **3b** is deposited from dichlorobenzene (DCB) instead of water:DMSO, epitaxially adsorbed fibrils are observed that aggregate to form assemblies that range from 4.6–6.4 nm (Figure 4d i,ii). Modeling suggests that in order to match the smaller spacings, interdigitation of alkyl tails of **3b** would have to occur and the guanines form the Tape II motif (see Supp. Info.). The less ordered nature of these assemblies from DCB suggests that in this non-H bonding solvent, large fibrillar aggregates form in solution first and are then adsorbed on the surface. This is consistent with the ability of **3b** (and related compounds) to form gels in non-H-bonding solvents.[13] Thus, by changing the solvent conditions, which alters the nature of the supramolecular interactions, dramatic differences in the resulting surface growth and assemblies can be observed.[14]

Conclusions

Access to tailored surface assemblies relies on the ability to control both surface-adsorbate and adsorbate-adsorbate interactions. We have demonstrated herein that hierarchical surface needle-like assemblies can be accessed through controlling the adsorbate-adsorbate interactions along different axes by simply changing the nature of the assembling monomer from ditopic to monotopic. Using fluid tapping mode AFM we have been able to observe in real-time the growth of these assemblies, and while the growth rates estimated by these studies may not be quantitative, especially in comparison to experiments carried out under even slightly different conditions, they do highlight the anisotropic nature of the assemblies formed under these specific experimental conditions. Furthermore, through judicious solvent selection, chosen to influence adsorbate-adsorbate and surface-adsorbate interactions, the nature of the assemblies can be dramatically altered. Deposition from aqueous solutions hinders the formation of hydrogen bonded aggregates in solution and thus encourages adsorption onto the surface before hydrogen bonded assemblies can occur. However, deposition from a non-hydrogen bonding solvent will allow hydrogen bonded aggregates to form in solution thus resulting in the adsorption of aggregates on the surface rather than the adsorption of single monomers. This can result in the formation of different types of hydrogen bonded aggregates forming on the surface. Utilization of such concepts can be powerful tools in designing and accessing more controlled nano-assemblies at the interface.

Supplementary Material

Refer to Web version on PubMed Central for supplementary material.

Acknowledgements

This material is based upon work supported by the National Institutes of Health under grant Nos. NIBIB-EB-001466 and EB-002067, the National Science Foundation under grant no. MWN DMR-0602869 and by the Case MSTP (T32 GM07250).

REFERENCES

1. For example, see:(a) Schönherr H, Paraschiv V, Zapotoczny S, Crego-Calama M, Timmerman P, Frank CW, Vancso GJ, Reinhoudt DN. Proc. Natl. Acad. Sci 2002;99:5024–5027. [PubMed: 11929980] (b) Michl J, Magnera TF. Proc. Natl. Acad. Sci 2002;99:4788–4792. [PubMed: 11959931] (c) Theobald JA, Oxtoby NS, Phillips MA, Champness NR, Beton PH. Nature 2003;424:1029–1031. [PubMed:

12944962] (d) Ryu DY, Shin K, Drockenmuller E, Hawker CJ, Russell TP. Science 2005;308:236–239. [PubMed: 15821087] (e) Barth JV, Costantini G, Kern K. Nature 2005;437:671–679. [PubMed: 16193042] (f) Surin M, Samori P, Jouaiti A, Kyritsakas N, Hosseini MW. Angew. Chem. Int. Engl 2007;46:245–249. (g) Kampschulte L, Werblowsky TL, Kishore RSK, Schmittel M, Heckl WM, Lackinger M. J. Am. Chem. Soc 2008;130:8502–8507. [PubMed: 18533654]

2. For some recent reviews see:(a) Tao F, Bernasek SL. Chem. Rev 2007;107:1408–1453. [PubMed: 17439290] (b) Barth JV. Ann. Rev. Phys. Chem 2007;58:375–407. [PubMed: 17430091] (c) Wan L-J. Acc. Chem. Res 2006;39:334–342. [PubMed: 16700532] (d) Humblot V, Barlow SM, Raval R. Prog. Surf. Sci 2004;76:1–19. (e) De Feyter S, De Schryver FC. Chem. Soc. Rev 2003;32:139–150. [PubMed: 12792937]
3. Israelachvili, J. Intermolecular and Surface Forces. London: Academic Press Limited; 1992. p. 238-239.
4. (a) De Feyter S, Gesquière A, Klapper M, Müllen K, De Schryver FC. Nano Lett 2003;3:1485–1488. b) De Feyter S, De Schryver FC. J. Phys. Chem. B 2005;109:4290–4302. [PubMed: 16851494] c) Klymchenko AS, Furukawa S, Müllen K, Van der Auweraer M, De Feyter S. Nano Lett 2007;7:791–795. [PubMed: 17309319]
5. (a) Groszek AJ. Proc. Roy. Soc. Lond. A 1970;314:473–498. (b) Leunissen ME, Graswinckel WS, Enckevort WJP, Vlieg E. Cryst. Growth Des 2003;4:361–367.
6. (a) Cyr DM, Venkataraman B, Flynn GW. Chem. Mater 1996;8:1600–1615. (b) Holland NB, Ruegsegger M, Marchant RE. Langmuir 1998;14:2790–2795. (c) Hibino M, Sumi A, Hatta I. Thin Solid Films 1996:281–282. 594–597. (d) Eichhorst-Gerner K, Stabel A, Moessner G, Declerq D, Valiyaveettil S, Enkelmann V, Müllen K, Rabe JP. Angew. Chem. Int. Ed 1996;35:1492–1495. (e) Stabel A, Heinz R, Rabe JP, Wegner G, De Schryver FC, Corens D, Dehaen W, Süling C. J. Phys. Chem 1995;99:8690–8697. (f) Fang H, Giancarlo LC, Flynn GW. J. Phys. Chem. B 1998;102:7311–7315.
7. (a) Jatsch A, Kopyshev A, Mena-Osteritz E, Bauerle P. Org. lett 2008;10:961–964. [PubMed: 18260670] (b) Piana S, Bilic A. J. Phys. Chem. B 2006;110:23467–23471. [PubMed: 17107199] (c) Perdigao LMA, Staniec PA, Champness NR, Kelly REA, Kantorovich LN, Beton PH. Phys. Rev. B 2006;73:195423/1–195423/7. (d) Kawai T, Tanaka H, Nakagawa T. Surf. Sci 1997;386:124–136. (e) Heckl WM, Smith DP, Binnig G, Klagges H, Hansch TW, Maddocks . J. Proc. Nat. Acad. Sci. USA 1991;88:8003–8005.
8. (a) Xu S, Dong M, Rauls E, Otero R, Linderoth TR, Besenbacher F. Nano Lett 2006;6:1434–1438. [PubMed: 16834424] (b) Mamdouh W, Dong M, Xu S, Rauls E, Besenbacher F. J. Am. Chem. Soc 2006;128:13305–13311. [PubMed: 17017813] (c) Mamdouh W, Dong M, Kelly REA, Kantorovich LN, Besenbacher F. J. Phys. Chem. B 2007;111:12048–12052. [PubMed: 17918893] (d) Xu W, Kelly REA, Otero R, Schock M, Loegsgaard E, Stensgarrd I, Kantorovich LN, Besenbacher F. Small 2007;3:2011–2014. [PubMed: 18022892] (e) Mamdouh W, Kelly REA, Dong M, Kantorovich LN, Besenbacher F. J. Am. Chem. Soc 2008;130:695–702. [PubMed: 18072777]
9. (a) Gottarelli G, Masiero S, Mezzina E, Pieraccini S, Rabe JP. Chem. Eur. J 2000;6:3242–3248. (b) Kelly REA, Kantorovich LN. J. Mater. Chem 2006;16:1894–1905.
10. (a) Kumar AMS, Sivakovac S, Marchant RE, Rowan SJ. Small 2007;3:783–787. [PubMed: 17385210] (b) Kumar AMS, Sivakova S, Fox JD, Green JE, Marchant RE, Rowan SJ. J. Am. Chem. Soc 2008;130:1466–1476. [PubMed: 18177047]
11. (a) Weckesser J, De Vita A, Barth JV, Cai C, Kern K. Phys. Rev. Lett 2001;87:096101.1–096101.4. [PubMed: 11531578] (b) Yokoyama T, Yokoyama S, Kamikado T, Okuno Y, Mashiko S. Nature 2001;413:619–621. [PubMed: 11675782]
12. Lena S, Brancolini G, Gottarelli G, Mariani P, Masiero S, Venturini A, Palermo V, Pandoli O, Pieraccini S, Samori S, Spada GP. Chem. Eur. J 2007;13:3757–3764.
13. Giorgi T, Grepioni F, Manet I, Mariani P, Masiero S, Mezzina E, Pieraccini S, Saturni L, Spada GP, Gottarelli G. Chem. Eur. J 2002;8:2143–2152.
14. Tao F, Bernasek SL. Langmuir 2007;23:3513–3522. [PubMed: 17328563]

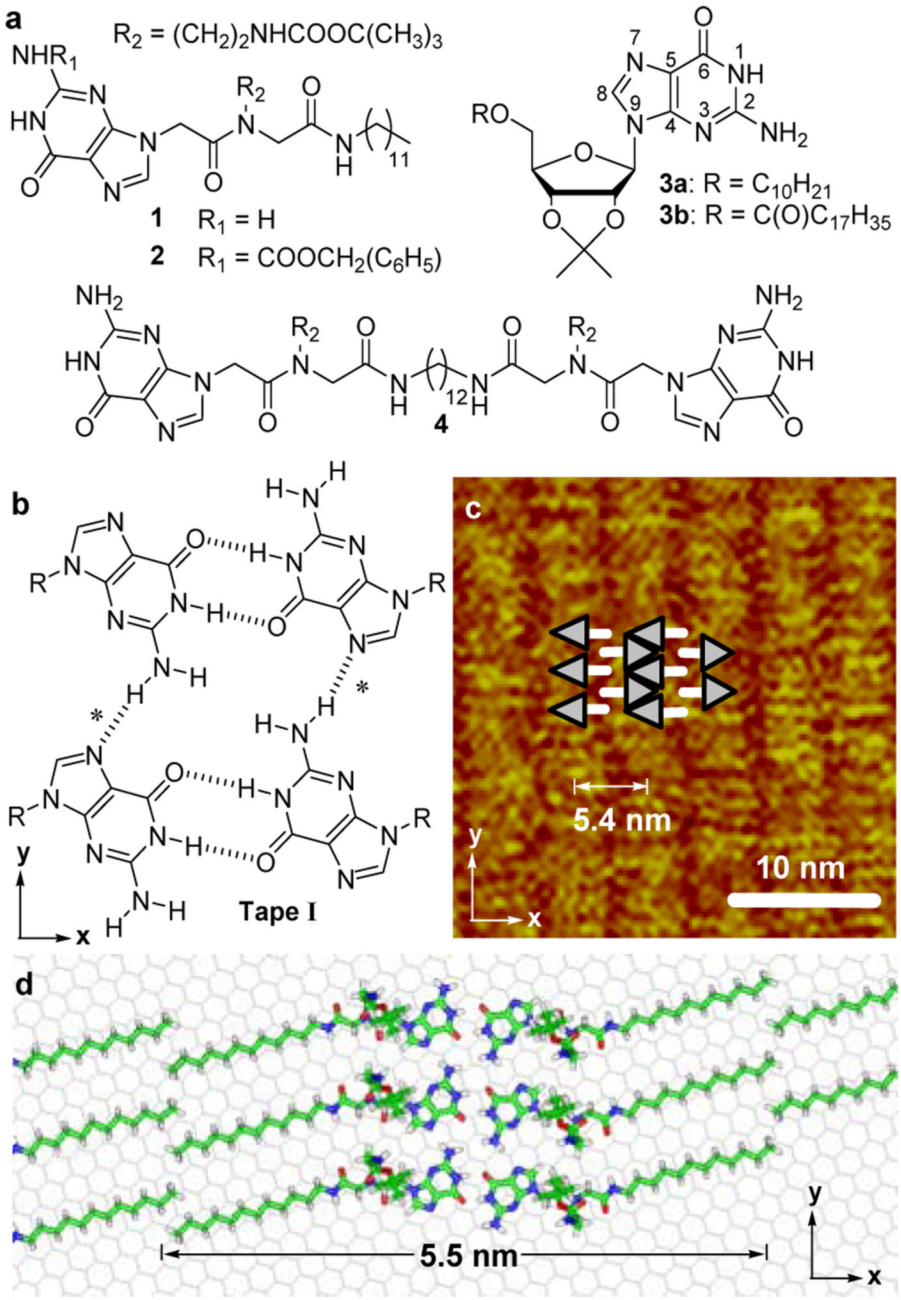

Figure 1.

a) Structures of compounds **1–4**. b) Proposed double-stranded guanine H-bonding motif (Tape I) with Watson-Crick (W/C) H-bonding dimers along the x-axis and inter-chain H-bonds (*) along the y-axis. c) AFM phase image of **1** assembled on HOPG with 5.4 ± 0.1 nm widths d) Energy minimized model of the assembly of **1** with matching widths.

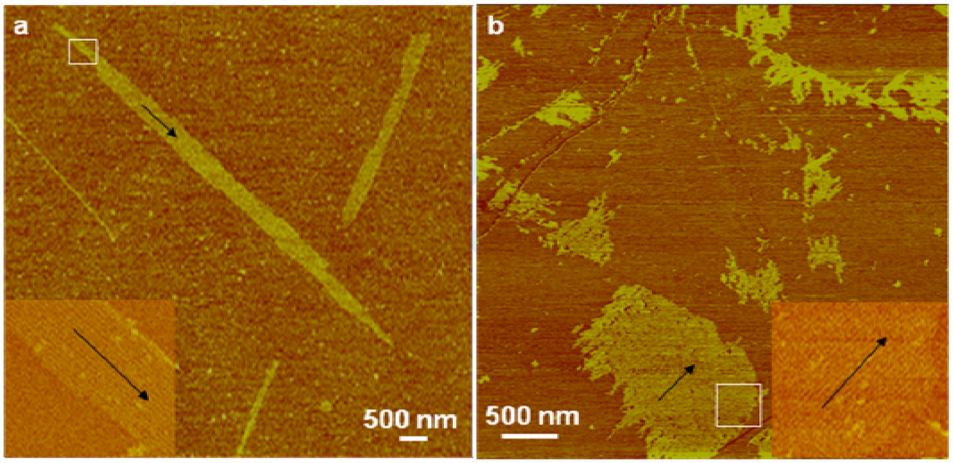

Figure 2.
AFM phase images of submonolayer assemblies of a) **1** forming high aspect ratio needle-like domains and b) **4** forming more block-like domains. Both **1** and **4** domains are composed of linear band structures (magnified insets). In the domains of **1**, the bands align along the length of the needle.

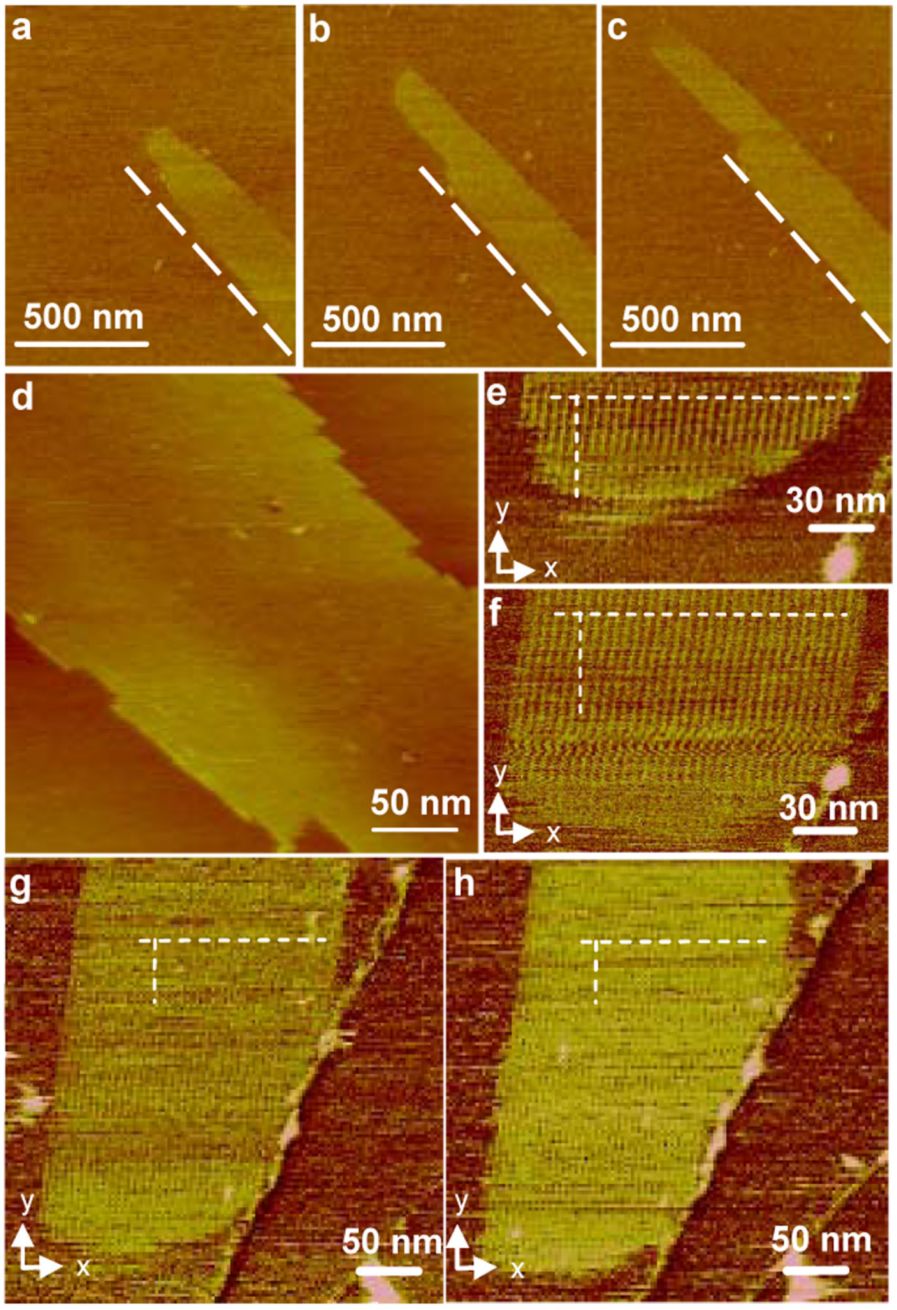

Figure 3.

AFM phase images of **1** assembling on HOPG from a water: DMSO (49:1) solution at a) t=0, b) t=5, c) t=10 mins from the start of scanning. d) Needle domain is composed of 5.4 ± 0.1 nm bands parallel to the length of the needle. AFM phase images of a second growing domain at e) t=0, f) t=5, g) t=10, h) t=13 mins. Markers (dashed lines) highlight the differences in the rate of assembly in this experiment along the y-axis (30 monomers/min) compared to the x-axis (3.0 monomers/min).

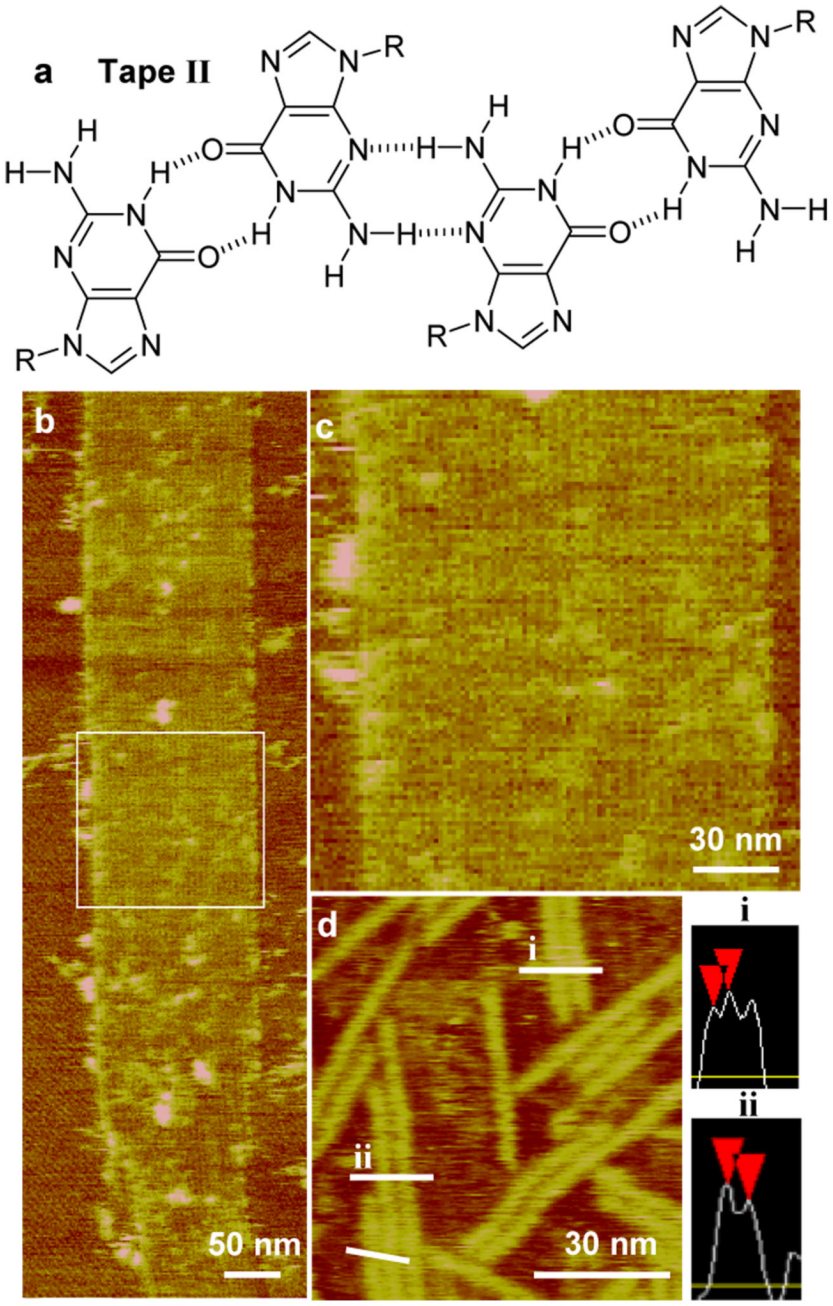

Figure 4.

a) An alternative centrosymmetric guanine H-bonding tape motif (Tape II). b) AFM image of a high aspect ratio assembly that results from depositing **3b** from water:DMSO (49:1), c) an expansion of box region in image b showing the banding pattern within these assemblies and d) AFM image of the assemblies obtained upon depositing **3b** from dichlorobenzene (DCB) solutions. Fibril spacing ranges from 4.6–6.4 nm: For example, (i) 5.8 nm, (ii) 4.7 nm.